Symmetry breaking effect on the inhomogeneous chiral transition in the magnetic field

R. Yoshiike and T. Tatsumi

Department of physics, Kyoto University, Kyoto 606-8502, Japan

We study the effect of the change of the current quark mass on the inhomogeneous chiral phase in the QCD phase diagram and discuss the properties of the phase transition using the generalized Ginzburg-Landau expansion. The strong external magnetic field spreads this phase over the low chemical potential region even if the current quark mass is finite. This implies that the existence of this phase can be explored by the lattice QCD simulation.

I. INTRODUCTION

Exploring the finite density region of the QCD phase diagram is one of the challenging issues in nuclear physics. Recently, the possible existence of the inhomogeneous chiral phase has been energetically discussed by the analysis of the Nambu-Jona-Lasinio (NJL)-type model [1–3] or the Shwinger-Dyson approach [4]. In this phase, the scalar and pseudoscalar quark condensates spatially modulate, and the complex order parameter, $\phi(\mathbf{r})$, representing this phase takes the form

$$\phi(\mathbf{r}) \equiv \langle\bar{\psi}\psi\rangle + i\langle\bar{\psi}i\gamma^5\tau_3\psi\rangle = \Delta(\mathbf{r})e^{i\theta(\mathbf{r})}. \quad (1)$$

As a definite form of $\phi(\mathbf{r})$, the dual chiral density wave (DCDW) $(\Delta(\mathbf{r}) = \Delta, \theta(\mathbf{r}) = qz)$ [1,4]; the real kink crystal (RKC) $(\Delta(\mathbf{r}) \sim \Delta\text{sn}(\boldsymbol{\kappa}z), \theta(\mathbf{r}) = 0)$, with the Jacobi elliptic function sn [2,3]; or the hybrid condensate $(\Delta(\mathbf{r}) \sim \Delta\text{sn}(\boldsymbol{\kappa}z), \theta(\mathbf{r}) = qz)$ [5] has been often used. These configurations can be obtained by using the Hartree-Fock solutions of the $1 + 1$-dimensional NJL(NJL$_2$) model in the chiral limit [6–8]. Most analyses have shown that the inhomogeneous chiral phase appears as an intermediate phase during the standard chiral phase transition.

Nowadays, various magnetic aspects of QCD have also attracted much interest because quark matter subjected to the strong magnetic field (B) is expected to occur in the early Universe, during the heavy ion collision $[B = \mathcal{O}(m_\pi^2 \sim 10^{17} \text{ G})]$ or in the core of compact stars $(B > 10^{12-15} \text{ G})$. Theoretically, the lattice QCD simulations have been done for the deconfinement transition or the chiral transition under the magnetic field with various strength. One of the interesting subjects there is the symmetry behavior in the presence of the magnetic field. It has been suggested that the chiral symmetry breaking is enhanced due to B in the effective model, *magnetic catalysis* [9–12]. However, the recent lattice simulations have shown *inverse magnetic catalysis* or *magnetic inhibition* [13,14]. This phenomenon is not well understood yet, and its origin is still controversial. It may be plausible that

some fluctuation effects become important, since the magnetic catalysis has been shown within the mean-field approximation. Recently, to explain this phenomenon within the effective models, an effective B-dependent four-Fermi coupling constant has been proposed. This dependence was introduced through the coupling of the quark or gluon loops to B perturbatively [15,16] or in the framework of functional renormalization group [17,18].

In the external magnetic field, the DCDW phase is remarkably extended in the low chemical potential (μ) region except for $\mu = 0$ [19]. The energy spectrum of the quark field exhibits the asymmetry, which gives rise to such distinctive behavior[1] [21]. Note that complex $\phi(\mathbf{r})$ is necessary for the energy spectrum to be asymmetric about zero. A peculiar role of the spectral asymmetry can be also seen around the transition point: it induces a new term in the thermodynamic potential, and consequently a new Lifshitz point (LP) should appear on the $\mu = 0$ line in the chiral limit [21]. If this is the case, one may expect a direct observation of DCDW by a lattice QCD simulations. The QCD phase diagram in the finite-μ region has been explored by the lattice QCD simulation, but its availability is severely restricted due to the sign problem. Some methods to overcome the sign problem have been proposed: for example, the Taylor expansion method [22,23], the reweighting method [24–27], the canonical approach [28–31], the analysis of Lee-Yang zero in QCD [32–34], and the analytic continuation method from imaginary chemical potentials [35–39]. However, these methods are limited in the high-temperature (T) region, $\mu/T < 1$ region. Therefore, if the inhomogeneous chiral phase develops in the low-μ region, we may have a chance to observe the existence of this phase by the lattice QCD simulation.

In the present work, we shall further discuss this issue in a realistic situation. We study the region around the phase

---

[1]In the recent paper, we have suggested a possibility of the spontaneous magnetization in the DCDW phase due to the spectral asymmetry [20].

transition by using the generalized Ginzburg-Landau (GL) expansion [3] with the finite current quark mass. The current mass is small but should be important below the low-energy scale of $\mathcal{O}(10^2)$ MeV, since it is well known that a pion mass of $\mathcal{O}(10^2)$ MeV is generated from the tiny current quark mass of several MeV. Thus, it is conceivable that the finite quark mass becomes very important in the vicinity of the critical point, where the wave number as well as the amplitude becomes very small. The current mass explicitly breaks chiral symmetry, and the energy degeneracy of states is lost under the symmetry operation; the degeneracy for $m \to -m(Z_2)$ in the case of RKC or that for $\theta \to \theta + \alpha(\text{const})$ [$U(1)$] is lost in the case of DCDW. Since we must utilize these states to construct the configuration of the order parameter together with spontaneously symmetry breaking (SSB), the current mass is expected to disfavor the appearance of the inhomogeneous chiral phase. For RKC, the exact solution can be obtained in the massive Gross-Neveu model [40], and the critical point has been demonstrated to be largely shifted [2] to reduce the phase region. For DCDW, although no exact solution is known, the effect of the current mass has been perturbatively discussed in Ref. [41]. They have found that the DCDW phase does not appear for the small coupling constant and the large current mass within the NJL model, while the DCDW phase appears for the same coupling constant in the chiral limit. However, the discussion may not be sufficient because any deformation of the DCDW form is not considered. To take into account the deformation, a variational method may work well [42]. Consequently, the effect of the current quark mass is almost similar to the case of RKC: the function form of DCDW is largely deformed near the transition point, and accordingly the DCDW region of the phase diagram is reduced. We shall follow the similar approach here and find the proper solution of $\theta(r)$ instead of qz near the transition point.

In particular, the effect of the finite current quark mass should be important when our idea is confronted with the lattice QCD simulations; one may also extract more information by changing its value by hand. We know that the LP resides on the $\mu = 0$ line in the chiral limit. Once the current mass is turned on, a competition arises between the positive effect on the DCDW phase by the magnetic field and the negative effect by the current mass. Consequently, the critical point should leave the $\mu = 0$ line, and some gap is formed between them. In contrast with the crossover for the usual chiral transition in the presence of the finite current mass, we shall see that the inhomogeneous transition should still have a clear phase boundary due to the loss of translational symmetry.

The paper is organized as follows. In Sec. II, we construct the thermodynamic potential by using the generalized GL expansion with the finite current quark mass, and the configuration of $\phi(\mathbf{r})$ is determined by the stationary condition. A peculiar role of the spectral asymmetry

of the quark energy eigenvalues is emphasized there. In Sec. III, the phase diagram of the DCDW phase is presented in the presence of the magnetic field, and some features of the phase transition are figured out around the transition point. The effect of the inverse magnetic catalysis is discussed there. The possibility of the observation is also discussed in the lattice QCD simulations, based on Ref. [43], where nonanalyticity of the partition function is studied in the DCDW phase. Section IV is devoted to a summary and concluding remarks.

II. THERMODYNAMIC POTENTIAL WITH FINITE CURRENT QUARK MASS

The thermodynamic potential near the transition point is given by the generalized GL expansion based on the NJL model [3]. The NJL model Lagrangian takes the form

$$\mathcal{L}_{\text{NJL}} = \bar{\psi}(i\not{D} - m_c)\psi + G[(\bar{\psi}\psi)^2 + (\bar{\psi}i\gamma^5\tau^a\psi)^2], \quad (2)$$

with the covariant derivative, $D_\mu = \partial_\mu + i\mathcal{Q}A_\mu$, where $\mathcal{Q}$ is the electric charge matrix in flavor space, $\mathcal{Q} = \text{diag}(e_u, e_d)$, and the $SU(2)$ symmetric quark mass, $m_c \equiv m_u = m_d \simeq 5$ MeV. We assume the mean field of the quark condensates,

$$M(\mathbf{r}) \equiv -2G\phi(\mathbf{r}) = me^{i\theta(z)}, \quad (3)$$

where $m = -2G\Delta$ plays a role of the dynamical quark mass, and the direction of modulation is taken to be parallel to the z axis. Then, the Lagrangian within the mean field approximation takes the form

$$\mathcal{L}_{\text{MF}} = \bar{\psi}[i\not{D} - m_c - m(\cos\theta(z) + i\gamma^5\tau^3\sin\theta(z))]\psi - \frac{m^2}{4G}. \quad (4)$$

Taking the external magnetic field **B** along the z axis, the thermodynamic potential can be written up to the fourth order about the order parameters and its derivative and the first order in m_c as

$$\Omega(\mu, T, B)$$
$$= \Omega_0 + \int \frac{d^3\mathbf{x}}{V}\left\{\alpha_1 m\cos\theta\right.$$
$$+ \frac{1}{2}\left(\alpha_2 + \frac{1}{2G}\right)m^2 + \tilde{\alpha}_2 m(\sin\theta)'$$
$$+ \frac{\alpha_3}{4}[4m^3\cos\theta - m(\cos\theta)''] + \tilde{\alpha}_3 m^2\theta'$$
$$+ \frac{\alpha_4}{4}(m^4 - m^2\theta\theta'') + 3\tilde{\alpha}_{4a}m^3(\sin\theta)'$$
$$\left. + \tilde{\alpha}_{4b}m(\sin\theta)''' \right\}, \quad (5)$$

with a shorthand notation, $\theta' \equiv \partial\theta/\partial z$, for given μ, T, and B. The GL coefficients read

$$\alpha_{2j} = (-1)^j 2N_c \sum_f T \sum_k \frac{|e_f B|}{2\pi} \sum_{n\geq 0}$$

$$\times \int \frac{dp}{2\pi} \frac{2 - \delta_{n,0}}{[(\omega_k + i\mu)^2 + p^2 + 2|e_f B|n]^j}, \quad (6)$$

$$\alpha_{2j-1} = m_c \alpha_{2j}, \quad (7)$$

$$\tilde{\alpha}_3 = N_c \sum_f \frac{|e_f B|}{16\pi^3 T} \mathrm{Im}\psi^{(1)}\left(\frac{1}{2} + i\frac{\mu}{2\pi T}\right), \quad (8)$$

$$\tilde{\alpha}_2 = m_c \tilde{\alpha}_3, \quad (9)$$

$$\tilde{\alpha}_{4b} = m_c N_c \sum_f \frac{|e_f B|}{1536\pi^5 T^3} \mathrm{Im}\psi^{(3)}\left(\frac{1}{2} + i\frac{\mu}{2\pi T}\right), \quad (10)$$

where $\omega_k = (2k+1)\pi T$ is the Matsubara frequency and Ω_0 is the constant term independent of the order parameters. The derivation of these equations is somewhat cumbersome and is relegated to Appendix A. Here, $\tilde{\alpha}_{4a}$ cannot be represented as a simple form (see Appendix A for details). Note that the effect of the current quark mass appears in α_{2j-1}, $\tilde{\alpha}_2$, $\tilde{\alpha}_{4a}$, and $\tilde{\alpha}_{4b}$, which are proportional to m_c. The coefficients $\alpha_i (i = 1-4)$ include an ultraviolet divergence and should be properly regularized by applying some regularization scheme. In the present calculation, the Pauli-Villars regularization (PVR) is used (Appendix B).

It may be worth mentioning that the $\tilde{\alpha}_3$ term originates from the spectral asymmetry of the quark energy eigenvalues and is proportional to B. The presence of such term has been shown in the chiral limit, and a close relation to the chiral anomaly has been demonstrated [21]. This argument can be easily generalized even if the current mass is taken into account (see Appendix C). Note that the $\tilde{\alpha}_3$ term remarkably extends the DCDW phase in the presence of the magnetic field [21], while it cannot appear in the RKC phase because of the absence of the phase degree of freedom.

The surface terms in Eq. (5) are irrelevant for the stationary condition: $\delta\Omega/\delta\theta(z) = 0$. Thus, we find the equation in the sine-Gordon form,

$$\theta'' + \mathrm{sign}(\alpha_1 + m^2\alpha_3)m_\pi^{*2} \sin\theta = 0, \quad (11)$$

with,

$$m_\pi^{*2} \equiv 2\frac{|\alpha_1 + m^2\alpha_3|}{m\alpha_4}, \quad (12)$$

and the relevant solution to Eq. (11) can be obtained as

$$\theta(z) = 2\mathrm{am}\left(\frac{m_\pi^*}{k}z, k\right) + \pi\theta(-\alpha_1 - m^2\alpha_3), \quad (13)$$

where "am" is the amplitude function with modulus $k \in [0, 1]$. Note here that the $\tilde{\alpha}_3$ term never affects the stationary condition; it plays instead an important role through the thermodynamic potential. Then, the period (l) and the wave number (Q) of condensates are defined by the relations

$$l = \frac{2kK(k)}{m_\pi^*}, \qquad Q = \frac{2\pi}{l} = \frac{\pi m_\pi^*}{kK(k)}, \quad (14)$$

where $K(k)$ is the complete elliptic integral of the first kind. There are two order parameters, m and k (or Q), where m characterizes the magnitude of SSB, and k measures a degree of the inhomogeneity. We plot the function $\pi + 2\mathrm{am}(x, k)$ in Fig. 1. When $k = 1$, Eq. (13) takes the form

$$\theta(z)|_{k=1} = 4\tan^{-1}(e^{m_\pi^* z}) - \pi\theta(\alpha_1 + m^2\alpha_3) \quad (15)$$

and behaves like the single kink. Accordingly, l diverges and Q vanishes because $K(k \to 1) \to \infty$. Then, we can see that the thermodynamic potential is reduced to the one in the homogeneous phase. On the other hand, when k and m_c simultaneously go to zero and $2m_\pi^*/k \to q$, Eq. (13) takes the form

$$\theta(z) \to qz + \pi\theta(-\alpha_1 - m^2\alpha_3), \quad (16)$$

and the original DCDW phase is recovered. In the following, we call the phase where $0 < k < 1$, $m \neq 0$, the *massive DCDW phase*.

Then, the thermodynamic potential takes the form

$$\Omega = \Omega_0 - |\alpha_1 m + \alpha_3 m^3|C_1(k) + \frac{1}{2}\left(\alpha_2 + \frac{1}{2G}\right)m^2$$

$$+ \tilde{\alpha}_3\sqrt{2\frac{|\alpha_1 + m^2\alpha_3|}{\alpha_4}}m^{3/2}C_3(k) + \frac{\alpha_4}{4}m^4, \quad (17)$$
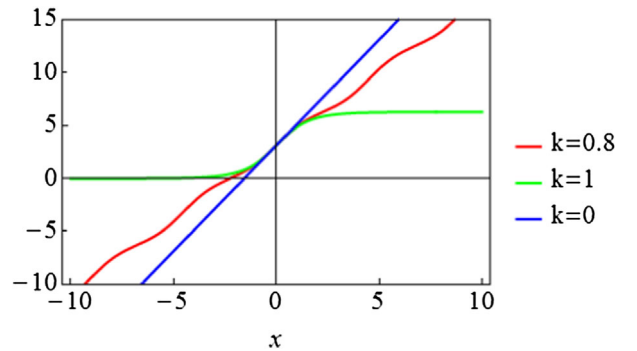

FIG. 1 (color online). Plot of $\pi + 2\mathrm{am}(x, k)$. The red, green, and blue lines describe the functions at $k = 0.8, 1, 0$, respectively.
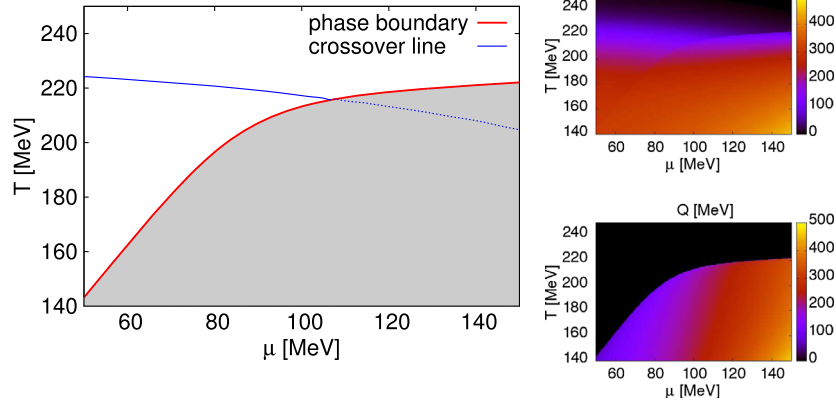
FIG. 2 (color online). Phase diagram at $m_c = 5$ MeV, $\sqrt{eB} = 1$ GeV (left panel). The red line describes the phase boundary between the massive DCDW phase (shaded area) and the homogeneous phase. The solid blue line describes the crossover line. The conventional crossover line without the massive DCDW phase corresponds to the dashed blue line. The right upper (lower) panel shows the value of m (Q) at the same range of $\mu - T$ as the left panel.

with

$$C_1(k) \equiv \frac{2}{k^2} - 1 - \frac{4E(k)}{k^2 K(k)}, \quad (18)$$

$$C_3(k) \equiv \frac{\pi}{kK(k)}, \quad (19)$$

where $E(k)$ is the complete elliptic integral of the second kind. Note that $\tilde{\alpha}_2, \tilde{\alpha}_{4a}, \tilde{\alpha}_{4b}$ terms vanish by the spatial integral. We can easily observe that Eq. (17) restored the thermodynamic potential in the homogeneous phase at $k \to 1$ because $C_1(k \to 1) = 1$ and $C_3(k \to 1) = 0$.

One may also find another possible solution of Eq. (11),

$$\theta_{os}(z) = 2\cos^{-1}[k' \text{sn}(m_\pi^* z, k')] + \pi\theta(-\alpha_1 - m^2\alpha_3), \quad (20)$$

with modulus $k' \in [0, 1]$. The previous solution (13) is the monotonically increasing function, while this solution is the oscillating function. Then, the thermodynamic potential takes the form

$$\Omega = \Omega_0 - |\alpha_1 m + \alpha_3 m^3| C_1^{os}(k') + \frac{1}{2}\left(\alpha_2 + \frac{1}{2G}\right)m^2$$

$$+ \frac{\alpha_4}{4}m^4, \quad (21)$$

with

$$C_1^{os}(k') \equiv 3 - 2k'^2 - \frac{4E(k')}{K(k')}. \quad (22)$$

When $k' = 1$, the solution (20) corresponds to $\theta(z)|_{k=1}$, and the thermodynamic potential becomes the one in the homogeneous phase. However, we can see that the oscillating solution is never favored compared to the homogeneous solution because $C_1^{os}(k') \leq C_1^{os}(k' = 1)$. Therefore, the

phase with the oscillating solution does not appear in the present situation.[2]

III. RESULTS AND DISCUSSIONS

A. Phase diagram around the transition point

For obtaining the phase diagram, the order parameters are determined to minimize Eq. (17). In the following, Q is used as the order parameter characterizing the inhomogenity instead of k. In the present calculation, we use the parameter set in Ref. [44], $\Lambda = 851$ MeV and $G\Lambda^2 = 2.87$, which reproduce pion decay constant $f_\pi = 93$ MeV, pion mass $m_\pi = 135$ MeV, and scalar condensate $\langle \bar{\psi}\psi \rangle = (-250 \text{ MeV})^3$ in the vacuum with $m_c = 5.2$ MeV.

In Fig. 2, we show the resulting phase diagram at $m_c = 5$ MeV, $\sqrt{eB} = 1$ GeV. There are the phase boundary between the massive DCDW phase and the homogeneous phase and the crossover line constituted by the pseudocritical temperature (T_{pc}) defined as the peak of the chiral susceptibility: $-\partial m/\partial T$.

In Fig. 3, the change of the phase diagram is described when m_c or B changes. We can find out that the massive DCDW phase is extended to the low-μ region with the decrease of m_c. Then, the result in Ref. [21] is recovered in the chiral limit, $m_c = 0$, and it is expected that the crossing point of the phase boundary and the crossover line agrees with the LP in the chiral limit. On the other hand, B raises the critical temperature in the phase transition, which is consistent with the magnetic catalysis. In other words, the smaller m_c or the larger B becomes, the more widely the massive DCDW phase develops over the region: $\mu/T < 1$.

A dependence of the order parameters on T is shown in Fig. 4. The discontinuity in the both order parameters can

---

[2]The oscillating solution may be relevant near the critical point in the absence of the magnetic field, where the similar equation is derived for θ [42].
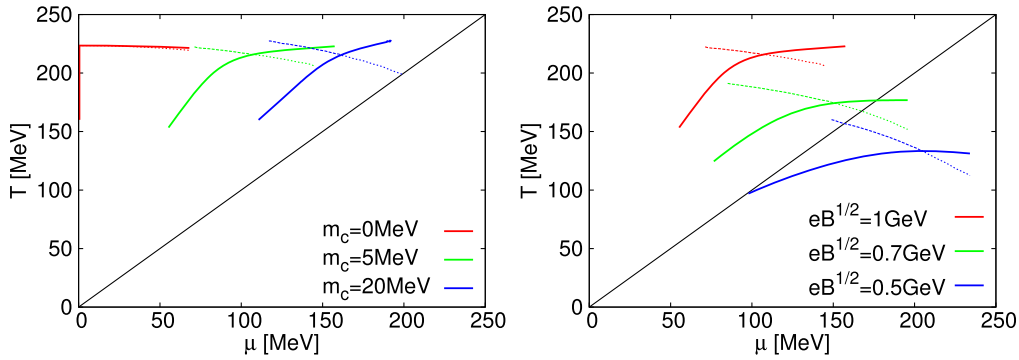
FIG. 3 (color online). Change of the phase boundary. In the left panel, the red, green, and blue lines describe the result at $m_c = 0, 5, 20$ MeV and fixed $\sqrt{eB} = 1$ GeV. In the right panel, the red, green, and blue lines describe the result at $\sqrt{eB} = 1, 0.7, 0.5$ GeV and fixed $m_c = 5$ MeV. The solid lines describe each phase boundary between the massive DCDW phase and the homogeneous phase. The dashed lines describe each crossover line.

be found at the critical temperature (T_c). Therefore, it can be concluded that there is a first-order phase transition between the massive DCDW phase (m is large and $Q \neq 0$) and the homogeneous phase (m is small but finite and $Q = 0$), though there is a second-order phase transition between the DCDW phase and the chiral-restored phase in the chiral limit [21]. The difference is caused by the finite m_c. In the chiral limit, Q can take any value in the chiral-restored phase since there is no condensate. On the other hand, the value of Q is uniquely determined in the case of the finite m_c because the condensate never vanishes there. In the right panel, we can see that the first-order phase transition is strong, while it becomes weaker for lower μ. The crossover between the homogeneously chiral-broken phase and the nearly restored phase is also observed at the pseudocritical temperature $T = T_{pc}$ in the left panel. The RKC or DCDW phase appears in the region $\mu \gtrsim 300$ MeV and $T \lesssim 50$ MeV with m_c and $B = 0$ [2,42]. However, we can see that B enlarges the massive DCDW phase over the low-μ and high-T region even if m_c is finite. Furthermore, the dynamical quark mass in the massive DCDW phase is larger than the

conventional one, and they coincide after the phase transition. In other words, the chiral symmetry breaking is enhanced in the massive DCDW phase. The fact may be consistent with the result in the chiral limit [21]: the chiral symmetry breaking is enhanced in the DCDW phase and the critical temperature is greater than the conventional one.

B. Effect of the inverse magnetic catalysis

In this subsection, the effect of the inverse magnetic catalysis is discussed in the present model. Here, it is assumed that the effect is described by giving a B dependence to the coupling constant of the NJL model (G). According to Ref. [45], G is fitted to reproduce the result of the lattice simulation [13,14]. For the parameter set, $\Lambda = 851$ MeV, $G\Lambda^2 = 2.87$, $m_c = 5$ MeV, the pseudocritical temperature can be obtained as $T_{pc}(eB = 0) = 173$ MeV at $\mu = B = 0$. In the following, we consider the case at $\sqrt{eB} = 1$ GeV. The coupling constant is put as $G\Lambda^2 = 1.85$, which gives the ratio $T_{pc}/T_{pc}(eB = 0) = 0.86$ at $\mu = 0$. In Fig. 5, the change of the phase boundary
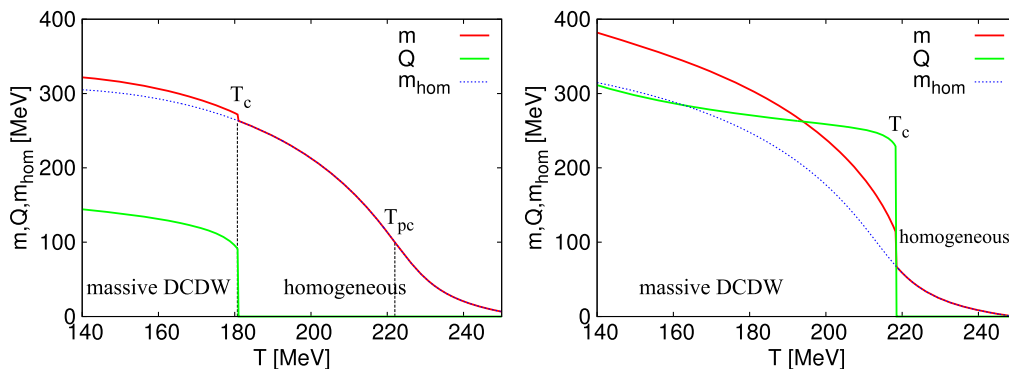

FIG. 4 (color online). Dependence of the order parameters on T for the same parameter set in Fig. 2. The red and green lines describe the amplitude m and the wave number Q, respectively. The dashed blue line shows the conventional dynamical quark mass without the inhomogeneous chiral condensate. The left panel shows the result at $\mu = 70$ MeV, and there are the phase transition point between the homogeneous phase and the massive DCDW phase on $T_c = 181$ MeV and the pseudocritical point on $T_{pc} = 222$ MeV. The right panel shows the result at $\mu = 120$ MeV, and there is the phase transition point on $T_c = 219$ MeV.
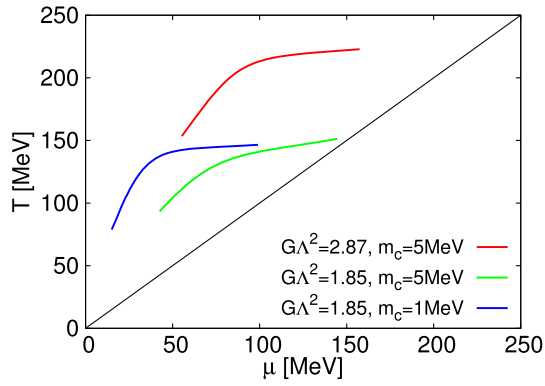
FIG. 5 (color online). Phase boundary obtained including the inverse magnetic catalysis. The red line corresponds to the phase boundary in the Fig. 2. On the other hand, the green and blue lines describe one at $m_c = 5, 1$ MeV with the inverse magnetic catalysis.

by the inverse magnetic catalysis is shown. The region of the massive DCDW phase shrinks, and the phase transition temperature decreases due to this effect. However, the massive DCDW phase remains in the $\mu/T < 1$ region if m_c is sufficiently small.

C. Possibility of the observation of the inhomogeneous chiral phase

In Ref. [43], the possibility of the observation of the DCDW phase has been discussed in the case with the singular line at $\mu = 0$. Though the existence of the line is pointed out by the generalized GL expansion with B in the chiral limit [21], the phase boundary is moved to the $\mu \neq 0$ region due to the current quark mass. The discussion becomes somewhat simple in the present case. In the Taylor expansion method, some quantity is expanded around $\mu/T = 0$ for considering the effect of the finite μ. Therefore, this method cannot describe the singularity at $\mu \neq 0$, and the massive DCDW phase cannot be grasped. For the same reason, the analytic continuation method from the imaginary chemical potential to the real one does not work, either. In other words, the applicable region of these methods is extremely restricted for the massive DCDW phase.

The reweighting method can overcome the difficulty of the singularity, in principle. In this method, the importance sampling is carried out for some parameter choice, for example, Re $\mu = 0$, where there is no sign problem. However, the massive DCDW phase does not develop in that region. Therefore, we need to find a special region with the massive DCDW phase and no sign problem there.

In the canonical approach, the problem of the singularity is irrelevant and the grand canonical potential with the real μ can be constructed from the one with the imaginary μ. If there is a massive DCDW phase in the $\mu \neq 0$ region, it may be found that the quark number density has the discontinuity derived from some first-order phase transition. However, the phase transition cannot be identified as one from the homogeneous

phase to the massive DCDW phase. Therefore, we need to find some specific order parameters on the phase transition. There is a similar difficulty in the Lee-Yang zero analysis in QCD. The behavior of zeros of the partition function indicates the existence of some phase transition. However, we cannot distinguish the phase transition including the massive DCDW phase by their distribution.

We also comment on the two color lattice QCD(QC$_2$D). In the QC$_2$D, there is no sign problem because the quark determinant is always real even if the chemical potential is real and finite [46]. Therefore, the existence of the inhomogeneous chiral phase may be investigated by the usual Monte Carlo simulation. It is also thought that this analysis works without sufficiently small m_c. It will be discussed elsewhere [47].

IV. SUMMARY AND CONCLUDING REMARKS

We have discussed the inhomogeneous chiral phase at $B \neq 0$ and $m_c \neq 0$. In this paper, the thermodynamic potential around the phase transition is obtained by the generalized GL expansion based on the NJL model. It is found that B extends the massive DCDW phase over the low-μ region similar to the DCDW phase in the chiral limit though m_c tends to reduce this phase. Then, there is the first-order phase transition between the massive DCDW phase and the homogeneous phase. Furthermore, the chiral symmetry is strongly broken in this phase compared to the conventional homogeneous phase.

Within our analysis based on the NJL model, B seems to raise the critical temperature. A similar mechanism to the magnetic catalysis should lead to this behavior. So we adjust the coupling constant of the NJL model to estimate the qualitative influence of the inverse magnetic catalysis. As a consequence, the critical temperature decreases. However, the massive DCDW phase can develop in the region $\mu/T < 1$ if m_c is sufficiently small. Therefore, we suggest that the inhomogeneous chiral phase can be found by the lattice QCD simulations just by choosing some proper method, for example, the reweighting method or the canonical approach. Since there is little work where the local chiral condensate is discussed [48], it is challenging work to actually confirm the existence of the inhomogeneous chiral phase by the lattice QCD simulations.

On the other hand, the possibility of the massive DCDW phase in B is also interesting from the view of the phenomenology. It is thought that the quark matter including s-quarks exists with a strong magnetic field in neutron stars. Therefore, the phase structure of massive quark matter is needed to discuss properties of neutron stars. Though they assume the s-quark condensate to be homogeneous in the previous works [49,50], s-quarks may be inhomogeneously condensed in neutron stars. Since the analysis in this paper works only at high temperature, we need to investigate the growth of the massive DCDW phase at zero or low temperature.

ACKNOWLEDGMENTS

APPENDIX A: GENERALIZED GL EXPANSION OF THE THERMODYNAMIC POTENTIAL

In this Appendix, the thermodynamic potential is expanded about the order parameter and its derivative with $m_c \neq 0$ and the external magnetic field (B) along the z axis based on Nickel's work [3]. The thermodynamic potential of the NJL model in the mean field approximation takes the form

$$
\begin{aligned}
\Omega(\mu, T, B) &= -\frac{T}{V} \text{Tr}_{D,c,f,V} \text{Ln}[S_B^{-1} - (\text{Re}\tilde{M} + i\gamma^5 \tau^3 \text{Im}\tilde{M})] + \frac{|M|^2}{4G} \\
&= \Omega_0 - \frac{T}{V} \sum_{j \geq 1} \frac{1}{j} \text{Tr}_{D,c,f,V} [S_B(\text{Re}\tilde{M} + i\gamma^5 \tau^3 \text{Im}\tilde{M})]^j + \frac{|M|^2}{4G},
\end{aligned}
\tag{A1}
$$

with $\tilde{M} \equiv m_c + M(z)$, where $M(z)$ is given in the Eq. (3) and Ω_0 is independent of the order parameters. S_B corresponds to the propagator in the chiral limit,

$$
S_B = \frac{1}{i\not{D} + \mu\gamma^0}.
\tag{A2}
$$

Then, odd j parts always vanish by the Dirac trace. We need the expansion up to the fifth order about $\tilde{M}$ and its derivative to obtain the thermodynamic potential constituted by the terms up to the fourth order about M and its derivative and the first order in m_c. The thermodynamic potential is expanded into the form in $B = 0$ [51],

$$
\begin{aligned}
\Omega &= \Omega_0 + \int \frac{d^3\mathbf{x}}{V} \left\{ \frac{\alpha_2}{2} |\tilde{M}|^2 + \frac{\alpha_4}{4} [|\tilde{M}|^4 - \text{Re}(\tilde{M}\tilde{M}'')] + \frac{|M|^2}{4G} \right\} \\
&= \Omega_0 + \int \frac{d^3\mathbf{x}}{V} \left[\frac{\alpha_2}{2} (|M|^2 + 2m_c \text{Re}M) + \frac{\alpha_4}{4} (|M|^4 + 4m_c |M|^2 \text{Re}M + |M'|^2 - m_c \text{Re}M'') + \frac{|M|^2}{4G} \right] + \mathcal{O}(m_c^2),
\end{aligned}
\tag{A3}
$$

with the GL coefficients,

$$
\alpha_{2j} = (-1)^j 4 N_c N_f T \sum_k \int \frac{d^3\mathbf{p}}{(2\pi)^3} \frac{1}{[(\omega_k + i\mu)^2 + \mathbf{p}^2]^j}.
\tag{A4}
$$

Switching on B, the summation of the eigenstate and the energy spectrum in α_{2j} should change as

$$
4 N_c N_f \int \frac{d^3\mathbf{p}}{(2\pi)^3} \to 2N_c \sum_f \frac{|e_f B|}{2\pi} \sum_n \int \frac{dp_z}{2\pi} (2 - \delta_{n,0}),
\tag{A5}
$$

$$
\mathbf{p}^2 \to p_z^2 + 2|e_f B|n,
\tag{A6}
$$

where n represents the Landau levels. Furthermore, some odd-order terms are added. The third-order term is derived from a part of $j = 2$ in Eq. (A1),

$$
\begin{aligned}
&-\frac{T}{V} \frac{1}{2} \text{Tr}_{D,c,f,V} [S_B(\text{Re}\tilde{M} + i\gamma^5 \tau^3 \text{Im}\tilde{M})]^2 \\
&\to -\frac{T}{V} \frac{1}{2} N_c \sum_f \int d^4 x d^4 x' \text{tr}\{[\text{Re}\tilde{M}(x_3) + i\gamma_5 \sigma_f \text{Im}\tilde{M}(x_3)] S_B(x, x') \\
&\quad \times [\text{Re}\tilde{M}'(x_3) + i\gamma_5 \sigma_f \text{Im}\tilde{M}'(x_3)](x_3' - x_3) S_B(x', x)\} \\
&= N_c \sum_f \frac{|e_f B|}{16\pi^3 T} \text{Im}\psi^{(1)} \left(\frac{1}{2} + i\frac{\mu}{2\pi T} \right) \int \frac{d^3\mathbf{x}}{V} \text{Im}(\tilde{M}^* \tilde{M}') \\
&= \tilde{\alpha}_3 \int \frac{d^3\mathbf{x}}{V} [\text{Im}(M^* M') + m_c \text{Im}M'],
\end{aligned}
\tag{A7}
$$

with $\sigma_u = +1$, $\sigma_d = -1$. It is convenient to use S_B in the momentum representation [52,53]. The fifth-order terms are derived from a part of $j = 2$ in Eq. (A1),

$$-\frac{T}{V}\frac{1}{2}\mathrm{Tr}_{D,c,f,V}[S_B(\mathrm{Re}\tilde{M} + i\gamma^5\tau^3\mathrm{Im}\tilde{M})]^2$$

$$\rightarrow -\frac{T}{V}\frac{1}{2}N_c\sum_f\int d^4x d^4x'\mathrm{tr}\left\{[\mathrm{Re}\tilde{M}(x_3) + i\gamma_5\sigma_f\mathrm{Im}\tilde{M}(x_3)]S_B(x,x')\right.$$

$$\left.\times\frac{1}{6}[\mathrm{Re}\tilde{M}'''(x_3) + i\gamma_5\sigma_f\mathrm{Im}\tilde{M}'''(x_3)](x_3' - x_3)^3 S_B(x',x)\right\}$$

$$= N_c\sum_f\frac{|e_f B|}{1536\pi^5 T^3}\mathrm{Im}\psi^{(3)}\left(\frac{1}{2} + i\frac{\mu}{2\pi T}\right)\int\frac{d^3x}{V}\mathrm{Im}(\tilde{M}^*\tilde{M}''')$$

$$\sim \tilde{\alpha}_{4b}\int\frac{d^3x}{V}\mathrm{Im}M'''. \tag{A8}$$

From a part of $j = 4$,

$$-\frac{T}{V}\frac{1}{4}\mathrm{Tr}_{D,c,f,V}[S_B(\mathrm{Re}\tilde{M} + i\gamma^5\tau^3\mathrm{Im}\tilde{M})]^4$$

$$\rightarrow -\frac{T}{V}\frac{3}{4}N_c\sum_f\int d^4x d^4x' d^4x'' d^4x'''$$

$$\times\mathrm{tr}\{[\mathrm{Re}\tilde{M}(x_3) + i\gamma_5\sigma_f\mathrm{Im}\tilde{M}(x_3)]S_B(x,x')[\mathrm{Re}\tilde{M}(x_3) + i\gamma_5\sigma_f\mathrm{Im}\tilde{M}(x_3))]S_B(x',x'')$$

$$\times[\mathrm{Re}\tilde{M}(x_3) + i\gamma_5\sigma_f\mathrm{Im}\tilde{M}(x_3)]S_B(x'',x''')[\mathrm{Re}\tilde{M}'(x_3) + i\gamma_5\sigma_f\mathrm{Im}\tilde{M}'(x_3)](x_3''' - x_3)S_B(x''',x)\}. \tag{A9}$$

Here, we can see that only the $|\tilde{M}|^2\mathrm{Im}(\tilde{M}^*\tilde{M}') \sim m_c|M|^2\mathrm{Im}M' + 2m_c\mathrm{Re}M\mathrm{Im}(M^*M')$ term survives after taking the Dirac trace and integrating. Therefore, this term can be described as

$$\tilde{\alpha}_{4a}\int\frac{d^3x}{V}[|M|^2\mathrm{Im}M' + 2\mathrm{Re}M\mathrm{Im}(M^*M')], \tag{A10}$$

where the coefficient is written as $\tilde{\alpha}_{4a}$ for convenience. In summary, the thermodynamic potential to fourth order takes Eq. (5).

APPENDIX B: REGULARIZATION OF THE GL COEFFICIENTS

In this Appendix, the GL coefficients including divergence are regularized by PVR. For convenience, we introduce the function I_j and rewrite Eq. (6),

$$\alpha_{2j} = (-1)^j N_c\sum_f\frac{|e_f B|}{2\pi}I_j(0), \tag{B1}$$

where

$$I_j(\Lambda^2) \equiv 2T\sum_k\sum_{n\geq 0}\int\frac{dp}{2\pi}\frac{2 - \delta_{n,0}}{[(\omega_k + i\mu)^2 + E_n^2(\Lambda^2)]^j}, \tag{B2}$$

$$E_n(\Lambda^2) \equiv \sqrt{p^2 + \Lambda^2 + 2|e_f B|n}. \tag{B3}$$

Then, $I_1(0)$ and $I_2(0)$ should be regularized. Taking the Matsubara summation,

$$I_1 = \sum_{n\geq 0}\int\frac{dp}{2\pi}\frac{2 - \delta_{n,0}}{E_n}[1 - f_F(E_n + \mu) - f_F(E_n - \mu)], \tag{B4}$$

$$I_2 = \frac{1}{2}\sum_{n\geq 0}(2 - \delta_{n,0})$$

$$\times\int\frac{dp}{2\pi}\left\{\frac{1}{E_n^3}[1 - f_F(E_n + \mu) - f_F(E_n - \mu)]\right.$$

$$\left.+\frac{1}{E_n^2}[f_F'(E_n + \mu) + f_F'(E_n - \mu)]\right\}, \tag{B5}$$

where f_F is the Fermion distribution function. Therefore, the diverging vacuum part can be decomposed into the form

$$I_{1,\text{vac}} = \sum_{n \geq 0} \int \frac{dp}{2\pi} \frac{2 - \delta_{n,0}}{E_n}, \tag{B6}$$

$$I_{2,\text{vac}} = \frac{1}{2} \sum_{n \geq 0} \int \frac{dp}{2\pi} \frac{2 - \delta_{n,0}}{E_n^3}. \tag{B7}$$

Then, $I_1(0)$ and $I_2(0)$ are regularized as the following:

$$I_{1,\text{vac}}(0) \rightarrow I_{1,\text{vac}}(0) - 2I_{1,\text{vac}}(\Lambda^2) + I_{1,\text{vac}}(2\Lambda^2), \tag{B8}$$

$$I_{2,\text{vac}}(0) \rightarrow I_{2,\text{vac}}(0) - I_{2,\text{vac}}(\Lambda^2). \tag{B9}$$

Thus, all divergence of coefficients can be excluded.

APPENDIX C: Spectral asymmetry with m_c

In this Appendix, we show that the $\tilde{\alpha}_3$ term is derived from the spectral asymmetry and relevant to the chiral anomaly when the inhomogeneous chiral condensate has the degree of freedom of the phase. Generally, the quark number with the finite T is given as [21]

$$N = -\frac{1}{2}\eta_H + \int dE\rho(E) \left[\frac{\theta(E)}{1 + e^{\beta(E-\mu)}} - \frac{\theta(-E)}{1 + e^{-\beta(E+\mu)}} \right], \tag{C1}$$

where $\rho(E)$ is the density of state. The first term, which is called the Atiyah-Patodi-Singer η invariant, represents the anomalous particle number [54,55],

$$\eta_H = \lim_{s \to +0} \int dE\rho(E)\text{sign}(E)|E|^{-s}, \tag{C2}$$

and measures the extent of *spectral asymmetry* about zero. The second term (N_{nom}) corresponds to the normal particle number, and we rewrite it as the form including the summation of the Matsubara frequency,

$$N_{\text{nom}} = \frac{1}{2}\eta_H - \int dE\rho(E)T\sum_k \frac{1}{E - \mu - i\omega_k}. \tag{C3}$$

Here, we can see that the first term in (C3) cancels out the anomalous particle number. However, the information of the η invariant is not washed away since the infinite series reproduces the anomalous particle number at $\mu = T = 0$.

The local density of state takes the form

$$\rho(\mathbf{x}, E) = \frac{1}{\pi} \text{Imtr}_{D,f,c}[R(\mathbf{x}, E + i\epsilon)]$$

$$= -\frac{N_c}{\pi} \sum_f \frac{\partial}{\partial E} \text{Imtr}_D \langle \mathbf{x}| \ln(H - E - i\epsilon)|\mathbf{x}\rangle, \tag{C4}$$

with the resolvent: $R(\mathbf{x}, E) \equiv \langle \mathbf{x}|\frac{1}{H-E}|\mathbf{x}\rangle$. In the present model, Hamiltonian takes the form

$$H = \vec{\alpha} \cdot \mathbf{P} + \gamma^0 [m_c + m e^{i\gamma^5 \tau_3 \theta(\mathbf{r})}], \tag{C5}$$

where $\alpha_i = \gamma_0 \gamma_i$ and $\mathbf{P}$ is the covariant derivative. After the Weinberg transformation, $\psi \to \psi_W = e^{i\gamma^5 \tau_3 \theta(\mathbf{r})/2}\psi$, the Hamiltonian changes to $\tilde{H}$,

$$\tilde{H} = \tilde{H}_0 + \delta\tilde{H}, \tag{C6}$$

$$\tilde{H}_0 \equiv \vec{\alpha} \cdot \mathbf{P} + \gamma_0 m, \tag{C7}$$

$$\delta\tilde{H} \equiv \gamma^0 \left[m_c e^{-i\gamma^5 \tau_3 \theta(\mathbf{r})} - \frac{1}{2}\gamma^5 \tau_3 \vec{\gamma} \cdot \vec{\nabla}\theta(\mathbf{r}) \right]. \tag{C8}$$

Therefore, $\rho(\mathbf{x}, E)$ can be expanded to the form

$$\rho(\mathbf{x}, E) = \frac{N_c}{\pi} \sum_f \text{Imtr} \left\langle \mathbf{x} \left| \frac{1}{\tilde{H}_0 - E} \right| \mathbf{x} \right\rangle$$

$$- \frac{N_c}{\pi} \sum_f \frac{\partial}{\partial E} \text{Imtr} \left\langle \mathbf{x} \left| \frac{1}{\tilde{H}_0 - E - i\epsilon} \right| \mathbf{x} \right\rangle \delta\tilde{H}(\mathbf{x})$$

$$+ \mathcal{O}(\partial(\delta\tilde{H}), (\delta\tilde{H})^2), \tag{C9}$$

where the first term does not depend on θ. Here, $\langle \mathbf{x}|\frac{1}{\tilde{H}_0 - E - i\epsilon}|\mathbf{x}\rangle$ can be rewritten into the propagator decomposed over the Landau levels [21].

Then, the reading term proportional to $\partial\theta$ takes the form

$$\rho_{\partial\theta}(\mathbf{x}, E)$$

$$= -\frac{N_c}{4\pi^2} \sum_f |e_f B| \partial_z \theta(\mathbf{x}) \frac{\partial}{\partial E} \left[\frac{|E|}{\sqrt{E^2 - m^2}} \theta(|E| - m) \right]. \tag{C10}$$

From Eq. (C3), the part of the quark number generated by $\rho_{\partial\theta}$ takes the form

$$N_{\partial\theta} = \frac{N_c}{4\pi^2} \sum_f |e_f B| \int d^3\mathbf{x} \partial_z \theta(\mathbf{x}) \left\{ 1 + T \sum_k \int_0^\infty dy \right.$$

$$\times \left[\frac{1}{(\sqrt{y^2 + m^2} - \mu - i\omega_k)^2} \right.$$

$$\left. \left. + \frac{1}{(\sqrt{y^2 + m^2} + \mu + i\omega_k)^2} \right] \right\}, \tag{C11}$$

where the first term is derived from the surface term in the partial integral about E and we take $y = \sqrt{E^2 - m^2}$. Then, the second term can be expanded with respect to m^2. It can be seen that the m^0 part of the second term cancels out the first term, and the remnant of $N_{\partial\theta}$ takes the form

$$N_{\partial\theta} = -\frac{N_c}{16\pi^3 T}\sum_f |e_f B|\int d\mathbf{x}^3 \partial_z \theta(\mathbf{x})$$

$$\times \frac{\partial}{\partial\mu}\mathrm{Im}\psi^{(1)}\left(\frac{1}{2} + i\frac{\mu}{2\pi T}\right)m^2 + \mathcal{O}(m^4). \quad \text{(C12)}$$

From the thermodynamic relation, $N/V = -\partial\Omega/\partial\mu$, we can see that the $\tilde{\alpha}_3$ term is generated.

On the other hand, the result from the chiral anomaly [56] is recovered in the limit $m \to \infty$. Then, the second term in Eq. (C11) vanishes, and the first term is the very contribution of chiral anomaly. This limit is consistent with the case where there are no valence quarks argued in the Ref. [20]. Furthermore, substituting the configuration of θ (13), the quark number takes the form

$$N_{\partial\theta} \to \frac{N_c}{4\pi^2}\sum_f |e_f B|\frac{\pi m_\pi^*}{kK(k)}. \quad \text{(C13)}$$

For investigating the variation from the case of the chiral limit [21], we take $2m_\pi^*/k = q$, where q is the wave vector of the DCDW condensate. Then, it can be expanded with respect to $(m_\pi^*/q)^2$,

$$N_{\partial\theta} = \frac{N_c}{4\pi^2}\sum_f |e_f B|q\left[1 - 2\frac{m_\pi^{*2}}{q^2} + \mathcal{O}\left(\frac{m_\pi^{*4}}{q^4}\right)\right]. \quad \text{(C14)}$$

The second term represents the correction by the finite m_c because of $m_\pi^{*2} \sim m_c$. The result also implies that the spectral asymmetry has the correction $\mathcal{O}(m_c)$ although the exact energy spectrum cannot be obtained at the finite m_c.

[1] E. Nakano and T. Tatsumi, Phys. Rev. D **71**, 114006 (2005).

[2] D. Nickel, Phys. Rev. D **80**, 074025 (2009).

[3] D. Nickel, Phys. Rev. Lett. **103**, 072301 (2009).

[4] D. Muller, M. Buballa, and J. Wambach, Phys. Lett. B **727**, 240 (2013).

[5] K. Nishiyama, S. Karasawa, and T. Tatsumi, Phys. Rev. D **92**, 036008 (2015).

[6] G. Basar and G. V. Dunne, Phys. Rev. D **78**, 065022 (2008).

[7] G. Basar, G. V. Dunne, and M. Thies, Phys. Rev. D **79**, 105012 (2009).

[8] D. Ebert, N. V. Gubina, K. G. Klimenko, S. G. Kurbanov, and V. C. Zhukovsky, Phys. Rev. D **84**, 025004 (2011).

[9] S. P. Klevansky and R. H. Lemmer, Phys. Rev. D **39**, 3478 (1989).

[10] H. Suganuma and T. Tatsumi, Ann. Phys. (N.Y.) **208**, 470 (1991).

[11] V. Gusynin, V. Miransky, and I. Shovkovy, Nucl. Phys. **B462**, 249 (1996).

[12] A. S. Vshivtsev, B. V. Magnitsky, V. C. Zhukovsky, and K. G. Klimenko, Fiz. Elem. Chastits At. Yadra **29**, 1259 (1998) [Phys. Part. Nucl. **29**, 523 (1998)].

[13] G. S. Bali, F. Bruckmann, G. Endrödi, Z. Fodor, S. D. Katz, and A. Schäfer, Phys. Rev. D **86**, 071502 (2012).

[14] G. Endrodi, J. High Energy Phys. 07 (2015) 173.

[15] R. L. S. Farias, K. P. Gomes, G. Krein, and M. B. Pinto, Phys. Rev. C **90**, 025203 (2014).

[16] E. J. Ferrer, V. de la Incera, and X. J. Wen, Phys. Rev. D **91**, 054006 (2015).

[17] N. Mueller and J. M. Pawlowski, Phys. Rev. D **91**, 116010 (2015).

[18] J. Braun, W. A. Mian, and S. Rechenberger, arXiv: 1412.6025.

[19] I. E. Frolov, V. C. Zhukovsky, and K. G. Klimenko, Phys. Rev. D **82**, 076002 (2010).

[20] R. Yoshiike, K. Nishiyama, and T. Tatsumi, Phys. Lett. B **751**, 123 (2015).

[21] T. Tatsumi, K. Nishiyama, and S. Karasawa, Phys. Lett. B **743**, 66 (2015).

[22] C. R. Allton, M. Döring, S. Ejiri, S. J. Hands, O. Kaczmarek, F. Karsch, E. Laermann, and K. Redlich, Phys. Rev. D **71**, 054508 (2005).

[23] R. V. Gavai and S. Gupta, Phys. Rev. D **78**, 114503 (2008).

[24] Z. Fodor and S. Katz, Phys. Lett. B **534**, 87 (2002).

[25] Z. Fodor, S. Katz, and K. Szabo, Phys. Lett. B **568**, 73 (2003).

[26] Z. Fodor and S. Katz, J. High Energy Phys. 03 (2002) 014.

[27] Z. Fodor and S. Katz, J. High Energy Phys. 04 (2004) 050.

[28] A. Alexandru, M. Faber, I. Horvath, and K.-F. Liu, Phys. Rev. D **72**, 114513 (2005).

[29] S. Kratochvila and P. de Forcand, Phys. Rev. D **73**, 114512 (2006).

[30] P. de Forcand and S. Kratochvila, Nucl. Phys. B, Proc. Suppl. **153**, 62 (2006).

[31] A. Li, A. Alexandru, K.-F. Liu, and X. Meng, Phys. Rev. D **82**, 054502 (2010).

[32] I. Barbour and A. Bell, Nucl. Phys. **B372**, 385 (1992).

[33] A. Nakamura and K. Nagata, arXiv:1305.0760.

[34] K. Nagata, K. Kashiwa, A. Nakamura, and S. M. Nishigaki, Phys. Rev. D **91**, 094507 (2015).

[35] P. de Forcand and O. Philipsen, Nucl. Phys. **B642**, 290 (2002).

[36] P. de Forcand and O. Philipsen, Nucl. Phys. **B673**, 170 (2003).

[37] M. D'Elia and M.-P. Lombardo, Phys. Rev. D **67**, 014505 (2003).

[38] M. D'Elia and M. P. Lombardo, Phys. Rev. D **70**, 074509 (2004).

[39] H.-S. Chen and X.-Q. Luo, Phys. Rev. D **72**, 034504 (2005).

[40] O. Schnetz, M. Thies, and K. Urlichs, Ann. Phys. (Amsterdam) **321**, 2604 (2006).

[41] S. Maedan, Prog. Theor. Phys. **123**, 285 (2010).

[42] S. Karasawa and T. Tatsumi, arXiv:1309.6448.

[43] K. Kashiwa, T.-G. Lee, K. Nishiyama, and R. Yoshiike, arXiv:1507.08382.

[44] S. P. Klevansky, Rev. Mod. Phys. **64**, 649 (1992).

[45] M. Ferreira, P. Costa, O. Lourenćo, T. Frederico, and C. Providência, Phys. Rev. D **89**, 116011 (2014).

[46] J. B. Kogut, D. K. Sinclair, S. J. Hands, and S. E. Morrison, Phys. Rev. D **64**, 094505 (2001).

[47] K. Kashiwa, T.-G. Lee, and R. Yoshiike (unpublished).

[48] T. Iritani, G. Cossu, and S. Hashimoto, Phys. Rev. D **91**, 094501 (2015).

[49] J. Moreira, B. Hiller, W. Broniowski, A. A. Osipov, and A. H. Blin, Phys. Rev. D **89**, 036009 (2014).

[50] S. Carignano, E. J. Ferrer, V. d. l. Incela, and L. Paulucci, Phys. Rev. D **92**, 105018 (2015).

[51] Y. Hidaka, K. Kamikado, T. Kanazawa, and T. Noumi, Phys. Rev. D **92**, 034003 (2015).

[52] J. Schwinger, Phys. Rev. **82**, 664 (1951).

[53] A. Chodos, K. Everding, and D. A. Owen, Phys. Rev. D **42**, 2881 (1990).

[54] A. J. Niemi and G. W. Semenoff, Phys. Rep. **135**, 99 (1986).

[55] A. J. Niemi, Nucl. Phys. **B251**, 155 (1985).

[56] D. T. Son and M. A. Stephanov, Phys. Rev. D **77**, 014021 (2008).